[논 문] 한국재료학회지
Korean J. Mater. Res.
Vol. 30, No. 11 (2020)

https://doi.org/10.3740/MRSK.2020.30.11.595

Photoactive Layer Formation with Oven Annealing for a Carbon Electrode Perovskite Solar Cell

Kwangbae Kim and Ohsung Song†

Department of Materials Science and Engineering, University of Seoul,
163, Seoulsiripdae-ro, Dongdaemun-gu, Seoul 02504, Republic of Korea

(Received September 1, 2020 : Revised October 12, 2020 : Accepted October 12, 2020)

Abstract The photovoltaic properties of perovskite solar cells (PSCs) with a carbon electrode fabricated using different annealing processes are investigated. Perovskite formation (50 °C, 60 min) using a hot-plate and an oven is carried out on cells with a glass/fluorine doped TiO_2/TiO_2/ZrO_2/carbon structure, and the photovoltaic properties of the PSCs are analyzed using a solar simulator. The microstructures of the PSCs are characterized using an optical microscope, a field emission scanning electron microscope, and an electron probe micro-analyzer (EPMA). Photovoltaic analysis shows that the energy conversion efficiency of the samples fabricated using the hot-plate and the oven processes are 2.08% and 6.90%, respectively. Based on the microstructure of the samples and the results of the EPMA, perovskite is formed locally on the carbon electrode surface as the γ-butyrolactone (GBL) solvent evaporates and moves to the top of the carbon electrode due to heat from the bottom of the sample during the hot plate process. When the oven process is used, perovskite forms evenly inside the carbon electrode, as the GBL solvent evaporates extremely slowly because heat is supplied from all directions. The importance of the even formation of perovskite inside the carbon electrode is emphasized, and the feasibility of oven annealing is confirmed for PSCs with carbon electrodes.

Key words carbon electrode, perovskite solar cell, active layer, hot-plate, oven.

1. Introduction

Perovskite solar cells (PSCs) have a high energy conversion efficiency (ECE) of about 24 %, which is comparable to that of silicon solar cells. Because of this, PSCs have been considered as a promising future energy source since they were first reported in 2009. PSCs can be manufactured through a simple solution process, and studies are currently being conducted to enable their commercialization, owing to their high productivity.[1] However, the expensive polymer and precious metal materials used for the hole transfer layer (HTL) and electrode of existing PSCs are an obstacle to their commercialization, as they account for more than 50 % of the total cost of a PSC.[2]

For the commercialization of PSCs, a large number of studies on HTL-free carbon electrode devices have been reported, among which, studies to control the thickness and uniformity of the carbon electrode layer and to increase the penetration rate of the perovskite solution into the carbon electrode layer are actively being conducted.[3-5]

The uniformity and thickness of the carbon electrode, which can vary for different fabrication processes, are reported to have a great influence on the ECE of the final device. The carbon electrode coating process can be generally divided into the doctor blade process and the screen printing process. F. Zhang et al.[6] have reported an ECE of 8.31 % for a device comprised of glass/fluorine doped tin oxide (FTO)/TiO_2/perovskite with a carbon electrode coated using the doctor blade process. One issue with the doctor blade process is the difficulty in controlling the thickness of the carbon electrode layer.

A. Mei et al.[5] have reported an ECE of 12.8 %, which is an improvement relative to that of the doctor blade process, by producing a glass/FTO/TiO_2/ZrO_2/screen printed carbon structure and dropping a perovskite solution on the carbon layer. Since this report, the method of dropping perovskite solution after screen printing was extensively

†Corresponding author
E-Mail : songos@uos.ac.kr (O. Song, Univ. of Seoul)

studied and mainly employed for PSCs with a carbon electrode.

To increase the infiltration of the perovskite solution, H. Tao et al.[7] adopted a carbon electrode with an improved porosity by adding polystyrene spheres, which decompose at 325 °C, into the carbon paste used for coating and then performing heat treatment at 400 °C for 30 min. N. Santhosh et al.[8] reported an increase in the ECE by improving the penetration of the perovskite solution through the use of γ-butyrolactone (GBL) and 5-ammonium valeric acid iodide (5-AVAI) instead of dimethylformamide and dimethyl sulfoxide to reduce the viscosity of the perovskite solution.

One disadvantage of the carbon electrode layer is that it is more than 100 times thicker than a precious metal electrode in a conventional PSC. Furthermore, there is insufficient research on the conditions required for the fabrication of perovskite with a uniform thickness in all directions.

A standard hot plate, which has been used for the fabrication of conventional perovskites, can be used for the heat treatment of nano-level perovskites through heat conduction from the bottom. However, the effect of the formation of perovskite on a thick micro-level carbon electrode and the uniform heating of the entire device using an oven on the photovoltaic properties and microstructure of the carbon electrode are still unknown.

Therefore, in this study, we aim to observe the photovoltaic properties and microstructure of PSCs with a carbon electrode fabricated through the hot plate process using a bottom heat source, and the oven process with heat supplied from all directions.

2. Experimental Procedure

PSCs were fabricated by adsorbing perovskite onto substrates with a glass/FTO/TiO_2/ZrO_2/carbon structure, and their photovoltaic properties were compared.

Fig. 1 shows a schematic diagram of the fabricated carbon electrode. To implement the device, a blocking layer was fabricated on the cleaned glass/FTO substrate using a compact TiO_2 (SC-BT060, Sharechem Co) solution. Meso-TiO_2 was produced through the screen printing process using TiO_2 paste (Sharechem Co). To prepare the ZrO_2 layer, ZrO_2 paste was coated on the prepared glass/FTO/BL-TiO_2/Meso-TiO_2 through the screen printing process, and then it was sintered at 500 °C for 30 min. After coating glass/FTO/BL-TiO_2/meso-TiO_2/ZrO_2 with a carbon paste through the screen printing process, it was sintered at 400 °C for 30 min to produce the glass/FTO/BL-TiO_2/meso-TiO_2/ZrO_2/carbon sample.

A perovskite solution was prepared by mixing CH_3NH_3I (99 %, Dyesol), PbI_2 (99.99 %, Alfa Aesar), and 5-AVAI in GBL (Sigma-Aldrich). The perovskite solution was dropped onto the prepared glass/FTO/BL-TiO_2/Meso-TiO_2/ZrO_2/carbon sample. Thereafter, using either a hot plate (NDK-1K, AS ONE) or an oven (ON-1E, Jeio Tech), the PSC was fabricated by drying at a temperature of 50 °C for 60 min.

To determine the photovoltaic properties of the manufactured PSCs, their current-voltage (I-V) curves was measured using a solar simulator (PEC-L11, Peccell) and a potentiostat (CompactStat.h, Ivium). A 100 W Xenon lamp was used as the light source, and the analysis was performed under 1 sun (100 mW/cm^2). The short circuit current density (J_{sc}), open circuit voltage (V_{oc}), fill factor (FF), and ECE were obtained using the I-V curves.

Field emission scanning electron microscopy (FE-SEM S-4300, Hitachi Co.) at the acceleration voltage of 5 kV was used to observe the surface and cross-sectional microstructure of the carbon electrode-PSCs. To observe the elemental distribution of C, Zr, Pb, and I in the perovskite layer, the vertical section of the device was enlarged to 2.7 K in the line scanning mode of the electron probe micro analyzer (EPMA).

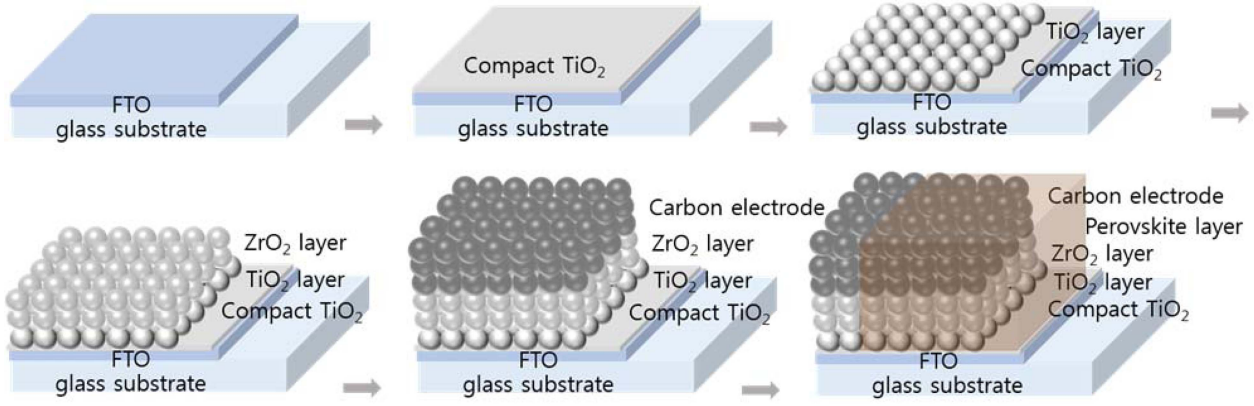

Fig. 1. Fabrication process of the carbon electrode PSC device.

3. Results and Discussion

Fig. 2 shows the I-V curves of the PSCs manufactured using the different heat treatments. Based on the I-V curve, the J_{sc}, V_{oc}, FF, and ECE of the fabricated devices were identified. The sample sintered in the oven had a higher ECE than that annealed on the hot plate, resulting in the excellent J_{sc} of the device manufactured using the oven.

The solvent drying method for the perovskite solution appeared to affect J_{sc}, thereby resulting in the difference between the ECE of the PSCs.

Table 1 shows the results of the property analyses on Fig. 2. The J_{sc} of the device sintered on the hot plate was 4.79 mA/cm^2, while that of the device sintered in the oven was 11.00 mA/cm^2, demonstrating a 2.3 fold increase. The V_{oc} of the devices with the same lower layer and electrode were equal, and there was about a 0.19 difference in the FF due to the difference in the J_{sc}. The ECE values of 2.08 % and 6.60 % were caused by the difference in J_{sc}.

Ultimately, the photovoltaic properties, especially the ECE, depended on the differences in J_{sc} during the formation of the perovskite layer. The higher ECE of the device sintered in the oven is due to the formation of a more uniform perovskite layer through the oven process compared to the hot plate process, which becomes engaged in relatively more photovoltaic reactions in the carbon electrode layer. In particular, the I-V curve of the sample prepared through the oven process showed a high current density of 12.57 mA/cm^2 at 0.45 V, which is a unique phenomenon in reported carbon electrode perovskite structures.[9)]

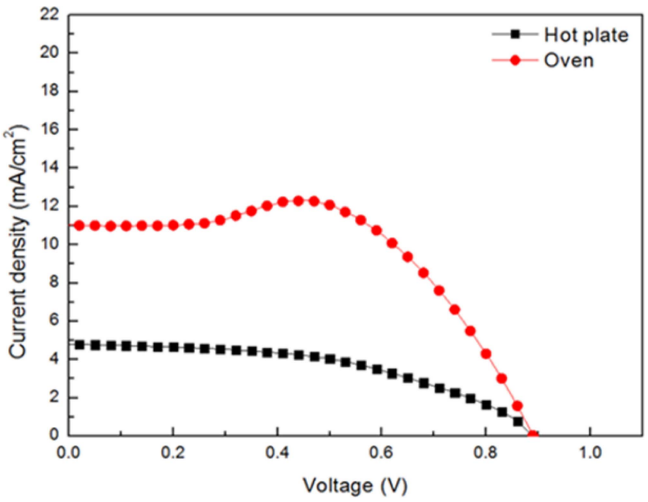

Fig. 2. I-V curves of PSCs fabricated using different heat treatment methods.

Table 1. Photovoltaic properties of PSCs with different heat treatment for perovskite formation.

Heat treatment	J_{sc} (mA/cm^2)	V_{oc} (V)	FF	ECE (%)
Hot plate	4.79	0.88	0.49	2.08
Oven	11.00	0.88	0.68	6.60

Fig. 3 shows the final in-plane images of the devices manufactured through the hot plate process and the oven process with the SEM images of the selected areas.

On the surface of the device prepared through the hot plate process, 50 μm-sized perovskite cubic crystals and 20 μm perovskite aggregates were observed, as shown in Fig. 3(a). As reported by Li et al.,[10)] perovskite tends to aggregate when the solvent fails to evaporate simultaneously at low temperatures.

On the surface of the device prepared through the oven process, as shown in Fig. 3(b), uniform micro perovskite crystals around 10 μm or less were found. A carbon layer in black was also observed among the perovskite layers.

With the same perovskite solution injected, the device prepared through the hot plate process, as shown in Fig. 3(a), had a relatively large amount of perovskite aggregates on the surface, while the device prepared through the oven process had a uniform micro perovskite layer on the surface, indicating that perovskite was uniformly formed along the direction of the thickness of the carbon electrode layer.

Fig. 4 shows the cross-sectional SEM images of the prepared devices. A low magnification image is shown on the left, and an enlarged image of the boxed area in the left image is shown on the right.

Fig. 4(a) shows the cross-section of the sample before the formation of the perovskite layer, in which a 500 nm FTO/500 nm TiO_2/1000 nm ZrO_2/17 μm meso carbon electrode layer were formed on the glass substrate. No cracks were found at each interface, and the top of the carbon electrode was relatively flat.

Fig. 4(b) shows the cross-section of the sample after the hot plate process. In the image on the left, no change was observed in the electron transport layer (ETL) composed of ZrO_2. 16.2 μm-thick aggregation of perovskite on the top of the carbon electrode, and 1um or larger width macrocracks which were formed during hot plate annealing were observed

From the magnified image on the right showing ETL and carbon electrode surface composed of ZrO_2, ETL in itself showed the same thickness with Fig. 4(a). However, both microcracks (<0.1 um) and macrocracks (>0.1 um) were observed in the carbon electrode layer near ETL.

Notably, there was a very large plate-like crack in the carbon layer above the ZrO_2 layer. The macrocracks in the carbon electrode layer caused a large increase in the

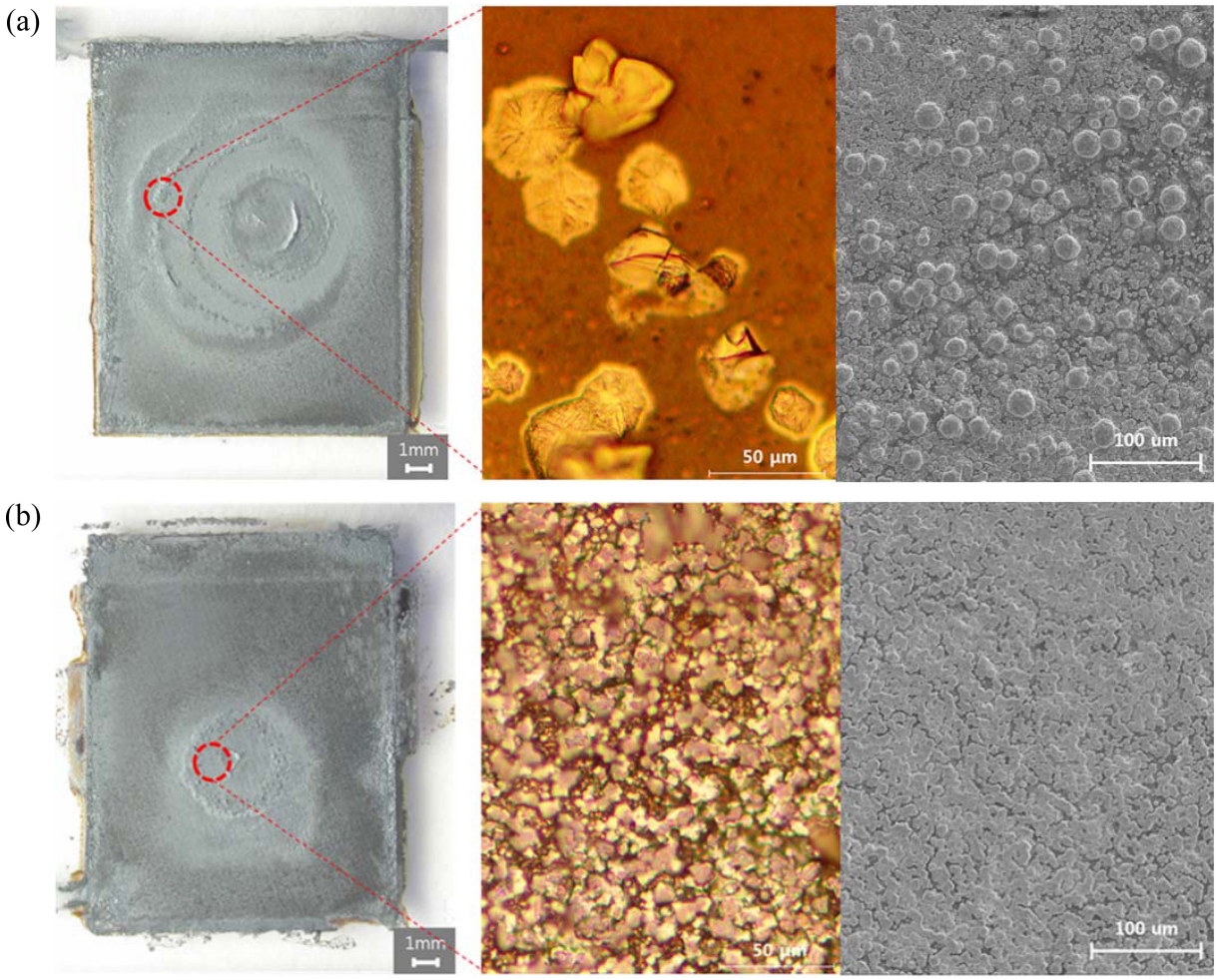

Fig. 3. Plane-view optical and SEM images of PSCs prepared through the (a) hot plate process and (b) oven process.

electric resistance during hole transport, resulting in the difference in the V_{oc} slope of the I-V curve as previously determined by the photovoltaic analysis. The result indicated an increase in the series resistance of the device.

Fig. 4(c) shows the cross-sectional image of the sample after the oven process. There was no significant change in thickness of the ETL. Unlike the device prepared through the hot plate process as shown in Fig. 4(b), a relatively uniform perovskite layer was formed after the oven process without causing any change in the thickness of the carbon electrode. However, microcracks, indicated dotted circles, were formed on the carbon electrode layer and perovskite layer as shown in the magnified image on the right.

These microcracks on the carbon electrode layer after the oven process may generate a hump of J_{SC} at 0.45 V as previously shown in the I-V graph of the oven process in Fig. 2. S. Hashmi et al.[9] reported the similar I-V result showing hump in carbon electrode PSC already. However, there was no graph showing hump by use of the original metal electrode. Microcracks formed inside the carbon electrode can be traps that delay the transfer of exiton. Change in hump over 0.35 V from the I-V graph might be caused by escape of the trapped exiton.[11]

Fig. 5 shows the results of the EPMA line scanning in the vertical section of the devices through the hot plate and the oven process as shown in Fig. 4.

Based on the Zr element analysis of the ZrO_2 layer, some distributions of constituent elements (Pb and I) of perovskite and of a constituent element (Carbon) of the carbon electrode were observed from the surface. Area of each layer was shown with a bar scale in the middle of the EPMA graph.

Fig. 5(a) shows the line scanning result of the device annealed with the hot plate process. As shown in Fig. 4, the perovskite was concentrated as 16.2 μm-thick agglomeration on the top of the carbon electrode. Low distribution of perovskite was confirmed due to the macrocracks created by formation of the perovskite in the middle of the carbon electrode. The non-uniform distribution on the carbon electrode was generated due to the macrocracks from the volume expansion during the

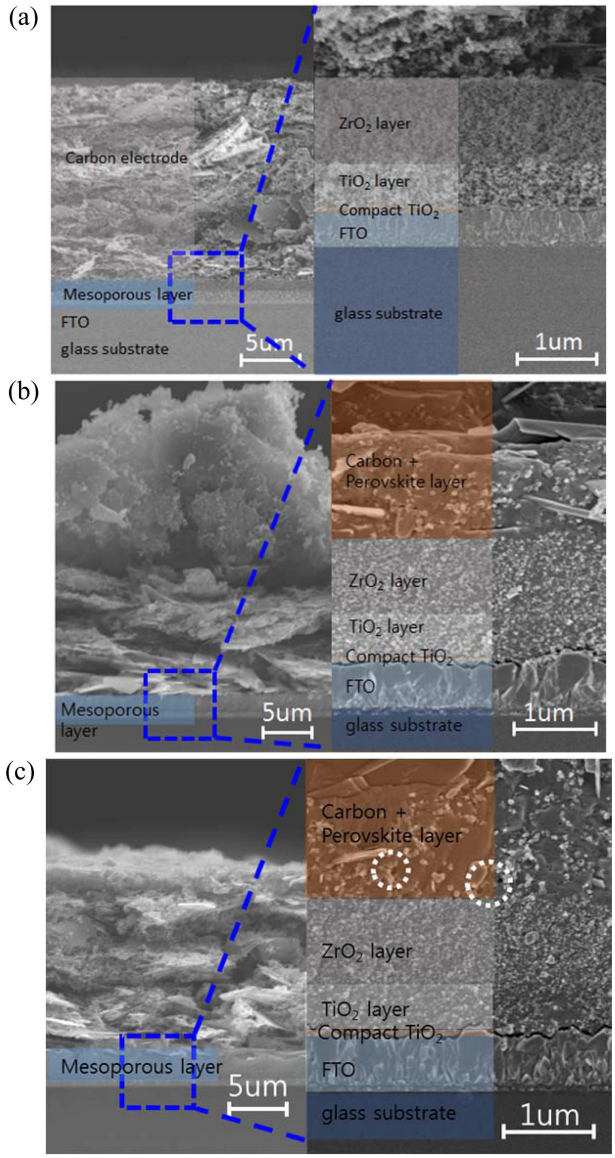

Fig. 4. Cross-sectional SEM images of the (a) as-prepared, (b) hot-plate treated, and (c) oven treated in PSCs.

perovskite formation process by the hot plate annealing.

Fig. 5(b) shows the line scanning result of the device manufactured through the oven process. Perovskite was uniformly formed along the direction of the thickness of the carbon electrode, which suggests that perovskite was also uniformly formed over the entire thickness of the carbon electrode, as indicated by the ECE and microstructure results.

The hot plate process resulted in the uneven formation of perovskite inside the carbon electrode, development of cracks in the carbon electrode, and decrease in the ECE due to aggregates that formed on the surface, while the devices prepared through the oven process exhibited a relatively uniform formation of perovskite over the entire thickness of the carbon electrode layer and a reduced occurrence of cracks, which ultimately contributed to the improvement of the ECE.

4. Conclusion

Two different heat treatment methods, the hot plate process and the oven process, for perovskite formation were employed to fabricate PSCs with a carbon electrode, and the photovoltaic properties and microstructures of each device were observed. The device prepared through the hot plate process showed cracks in the carbon electrode layer, as the perovskite layer was formed through a one-directional heat transfer from the bottom. Perovskite using hot plate was distributed unevenly, with aggregates around 50 μm in size on the surface, resulting in the low ECE of the PSC. Therefore, the oven process is more suitable for PSCs with a carbon electrode, as it supplies heat evenly from all directions to form a uniform perovskite layer all over the carbon electrode layer, thereby improving the photovoltaic properties of the resulting PSC.

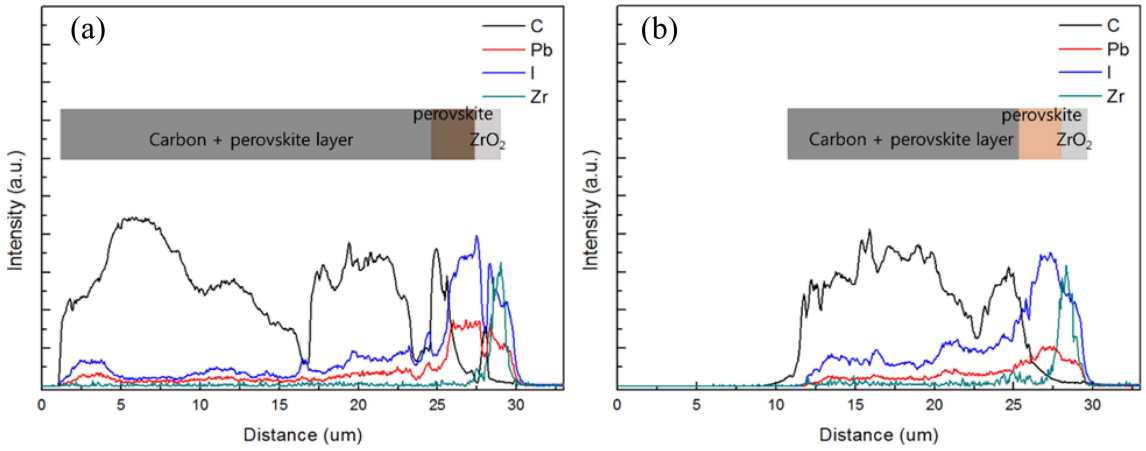

Fig. 5. Cross-sectional EPMA line scanning results of (a) hot-plate treated and (b) oven treated in PSCs.

Acknowledgement

This research was supported by Basic Science Research Program through the National Research Foundation of Korea (NRF) funded by the Ministry of Education (2017R1D1A1B03029347).

References

1. A. Kojima, K. Teshima, Y. Shirai and T. Miyasaka, J. Am. Chem. Soc., **131**, 6050 (2009).
2. S. Maniarasu, T. B. Korukonda, V. Manjunath, E. Ramasamy, M. Ramesh and G. Veerappan, Renew Sustain Energ. Rev., **82**, 845 (2018).
3. H. Zhou, Y. Shi, Q. Dong, H. Zhang, Y. Xing, K. Wang, Y. Du and T. Ma, J. Phys. Chem. Lett., **5**, 3241 (2014).
4. L. Zhang, T. Liu, L. Liu, M. Hu, Y. Yang, A. Mei and H. Han, J. Mater. Chem. A, **3**, 1965 (2015).
5. A. Mei, X. Li, L. Liu, Z. Ku, T. Liu, Y. Rong, M. Xu, M. Hu, J. Chen, Y. Yang and H. Han, Science, **345**, 295 (2014).
6. F. Zhang, X. Yang, H. Wang, M. Cheng, J. Zhao and L. Sun, ACS Appl. Mater. Interfaces, **6**, 16140 (2014).
7. H. Tao, Y. Li, C. Zhang, K. Wang, J. Wang, B. Tan, L. Han and J. Tao, Solid State Commun., **271**, 71 (2018).
8. N. Santhosh, S. R. Sitaaraman, P. Pounraj, R. Govindaraj, M. Senthil Pandian and P. Ramasamy, Mater. Lett., **236**, 706 (2019).
9. S. Hashmi, D. Martineau, M. Dar, T. Myllymaki, T. Sarikka, V. Ulla, S. Zakeeruddin and M. Gratzel, J. Mater. Chem. A, **5**, 12060 (2017).
10. Y. Li, Z. Zhao, F. Lin, X. Cao, X. Cui and J. Wei, Small, **13**, 1604125 (2017).
11. J. Li, Y. Wang, F. Wang, S. Liang, X. Lin, X. Chen and J. Zhou, Phys. Lett. A, **381**, 3732 (2017).

Author Information

Kwangbae Kim
Ph. D. Candidate, University of Seoul

Ohsung Song
Professor, University of Seoul